



Synthesis and Characterization of Chitosan/Cellulose Nanofibrils/Aspirin Composite Films

Ojo O.^{1,2} *, Maitera O. N.¹, Andrew F. P.¹, Yelwa J. M.^{3,**}

¹Department of Chemistry, Modibbo Adama University, Yola, Adamawa State, Nigeria

²Department of Chemistry, Federal College of Education (Tech) Gombe, Nigeria

³Department of Scientific and Industrial Research, National Research Institute for Chemical Technology, Zaria, Nigeria

*Corresponding author, Email address: [*molade80@gmail.com](mailto:molade80@gmail.com)

Corresponding author, Email address: mjyelwa@gmail.com

Received 01 Oct 2023,

Revised 20 Nov 2023,

Accepted 22 Nov 2023

Keywords:

- ✓ Drug delivery;
- ✓ Biopolymer,
- ✓ Optimisation;
- ✓ Polymer matrix;
- ✓ Transdermal;
- ✓ Sustainable materials

Citation: Ojo, O., Maitera O.N., Andrew F. P., Yelwa J.M. (2023) Synthesis And Characterization of Chitosan/Cellulose Nanofibrils/Aspirin Composite Films, *J. Mater. Environ. Sci.*, 14(11), 1245-1255

Abstract: In recent years, there has been a notable focus on the advancement of drug delivery systems with the objective of improving the effectiveness of therapeutic treatments and reducing the occurrence of adverse effects associated with pharmaceutical chemicals. The present study aimed to synthesise composite films consisting of chitosan-cellulose nanofibrils and aspirin, with the objective of developing a potentially effective drug loading platform. The synthesis procedure entailed dispersing cellulose nanofibrils in a chitosan solution, subsequently incorporating aspirin. Subsequently, the resultant combination was employed to fabricate films by the utilisation of a solvent evaporation procedure. The composite films were further subjected to characterization utilising a range of analytical techniques, including Fourier Transform Infrared Spectroscopy (FTIR), X-ray Diffraction (XRD), Transmission Electron Microscopy (TEM), Differential Scanning Calorimetry (DSC), Dynamic Light Scattering (DLS), and Thermogravimetric Analysis (TGA). The chemical interaction between cellulose and chitosan was confirmed using Fourier-transform infrared spectroscopy (FTIR), while the incorporation of cellulose nanofibrils into the chitosan matrix was observed through transmission electron microscopy (TEM) analysis. This resulted in the creation of a uniform and interconnected network structure. The utilisation of X-ray diffraction (XRD) facilitated the elucidation of the crystalline structure, while dynamic light scattering (DLS) provided valuable observations on the stability of colloidal systems. Differential scanning calorimetry (DSC) and thermogravimetric analysis (TGA) were employed to obtain thermal fingerprints, thereby facilitating the understanding of thermal transitions and stability. The optimisation of the composite for many applications, ranging from drug delivery systems to sustainable materials, was facilitated by this comprehensive characterization.

1. Introduction

In recent times, there has been an increasing scholarly focus on the advancement of innovative materials intended for the purpose of drug delivery systems (Akhter *et al.*, 2020). Biopolymers have emerged as significant components in the domains of materials science and biotechnology, marking the advent of a novel era characterized by the utilization of sustainable and biocompatible materials. Within this field, the synthesis and characterization of composites consisting of biopolymer cellulosic nanofibrils and chitosan emerge as a notable area of focus, showcasing significant innovation and potential. The composite material under consideration is formed by combining the unique characteristics of cellulose nanofibrils with chitosan, as described by Younes and Rinaudo in 2015. This combination results in a synergistic blend that significantly enhances its versatility, enabling its application in a wide range of contexts. Chitosan, a naturally occurring polysaccharide obtained from

chitin (Ramana *et al.*, 2014), and cellulose, a polymer that can be degraded by biological processes, exhibit distinctive characteristics that render them well-suited for drug encapsulation purposes (Liu *et al.*, 2018). Chitosan has potent antimicrobial properties, making it useful for antimicrobial agents in food, agriculture, anticorrosion and medical treatments (Sumaila *et al.*, 2022, Xing *et al.*, 2015; El Mouaden *et al.*, 2018; Akartasse *et al.*, 2022; Hemmingsen *et al.*, 2022). The process of creating composite films consisting of chitosan-cellulose nanofibrils and aspirin entails the amalgamation of chitosan and cellulose nanofibrils, subsequently integrating aspirin as the desired pharmaceutical agent (Huang *et al.*, 2018). Chitosan, due to its notable biocompatibility and biodegradability (Gadkari *et al.*, 2019), offers a suitable framework for the encapsulation of drugs (Casettari and Illum *et al.*, 2014; Hammi *et al.*, 2020; Zeyadi *et al.*, 2023). In contrast, cellulose nanofibrils possess notable attributes such as a high aspect ratio and a substantial surface area (Du *et al.*, 2019), which contribute to their improved mechanical strength and capacity for drug loading (Bhandari *et al.*, 2017). The characterization of these composite films holds significant importance in comprehending their physicochemical features and drug release behavior (Seah and Teo *et al.*, 2018). The evaluation of the films involves the utilization of several techniques, including transmission electron microscopy (TEM), Fourier-transform infra-red spectroscopy (FTIR), X-ray diffraction (XRD), and thermal analysis. These techniques are employed to assess the morphology, chemical composition, crystallinity, and thermal stability of the films. The potential of chitosan-cellulose nanofibrils/aspirin composite films in the domain of medication delivery is highly encouraging. According to Lu *et al.*, (2016), the use of chitosan and cellulose nanofibrils in conjunction presents a platform that is both biocompatible and biodegradable for the encapsulation of drugs. Furthermore, the inclusion of aspirin in this platform gives therapeutic advantages. Moreover, the films possess a high level of desirability for diverse biomedical applications due to their capacity to regulate drug release kinetics and augment antimicrobial efficacy (Shakya *et al.*, 2019). The objective of this study was to synthesize and characterize composite films consisting of chitosan-cellulose nanofibrils and aspirin for the purpose of drug loading. The comprehension of the physicochemical features and drug release behavior of these substances will play a significant role in the advancement of drug delivery systems that exhibit enhanced effectiveness and safety.

2. Methodology

2.1 Materials and Reagents

The sisal plant (*Agave Sisalana*) utilised in this research was procured from the Garkida Local Government Area in Adamawa State, Nigeria. It was subsequently identified by a botanist affiliated with Gombe State University, located in Gombe State, Nigeria. The necessary analytical grade reagents, such as Caustic soda (97% purity), fused calcium chloride, sulphuric acid (98% purity), hydrogen peroxide (50% purity), sodium sulphite, and sodium chlorite (80% purity), were acquired from Marcy Surgical Limited, located in Gombe, Gombe state. Additionally, aspirin (acetylsalicylic acid), ibuprofen, diclofenac, and chitosan were obtained from Cynco chemicals and Co, Ltd, situated in Lagos, Lagos state.

2.2 Research Methods

2.2.1 Cellulose Nanofibrils Extraction from *Agave sisalana*

The extraction of the cellulosic nanofibrils and the preparation of nanocomposites were performed using a method described by Sarkar *et al.*, (2017) with little modification.

2.2.2 Preparation of nanocomposite films

The nanocomposites were prepared in accordance with the formulation presented in the table below, which includes compositions comprising non-steroidal anti-inflammatory drugs (NSAIDs), such as aspirin. Various weight/percentage ratios of cellulosic nanofibrils (CNF) relative to the weight of chitosan were dispersed in a 30 ml solution of 3% (v/v) acetic acid. Additionally, 10% (w/w) of aspirin was introduced to the CNF dispersion. The solution obtained was subjected to sonication for a duration of 2 hours. Subsequently, a quantity of 1 gramme of chitosan was introduced into the dispersion of cellulose nanofibrils (CNF) within the drug solution, followed by agitation for a duration of 2 hours. The resulting solution was subsequently poured into Petri plates, where it was left to solidify for a duration of 1 hour at ambient temperature, followed by drying in an oven set at 500°C. The specimens were stored at ambient temperature prior to utilization.

Table 2. Formulation ratio of nanocomposite film based on chitosan/CNFs/aspirin

S/N	Composites Films	Formulation Ratio		
		Chitosan (%)	CNF (wt%)	Aspirin
1	F ₀	100	0.00	10
2	F ₁	100	0.25	10
3	F ₂	100	0.5	10
4	F ₃	100	0.75	10
5	F ₄	100	1.00	10

2.3 Characterisation

The morphology and size of the composite films were analysed using transmission electron microscopy (TEM). Fourier transform infrared spectroscopy (FTIR) was employed to determine the functional groups contained in the composite films. Additionally, X-ray diffraction (XRD), dynamic light scattering (DLS), differential scanning calorimetry (DSC), and thermogravimetric analysis (TGA) techniques were utilised

3. Results and Discussion

3.1 Fourier Transform Infrared Spectroscopy (FTIR)

The Fourier Transform Infrared (FTIR) spectra of the composite films consisting of chitosan-cellulose nanofibrils and aspirin exhibited distinct peaks that are indicative of specific molecular characteristics. Figure 1(a) displays the spectra of F₀ aspirin, revealing distinct absorption peaks at 3253 and 2885 cm⁻¹, which correspond to the stretching vibrations of O-H and C-H bonds, respectively. The infrared spectrum displays two distinct peaks at wavenumbers 1628 cm⁻¹ and 1543 cm⁻¹, which can be attributed to the amide I (C=O) and amide II (N-H) functional groups, respectively. Additionally, a peak at 1408 cm⁻¹ is observed, which corresponds to the vibrational mode of C-CH₃. In Figure 1 (b), the F₁ aspirin sample has a distinct peak at wavenumbers of 3492 cm⁻¹ and 2963 cm⁻¹, which correspond to the stretching vibrations of N-H and C-H bonds, respectively. The compound F₁ aspirin exhibits distinctive spectral peaks at 1751 cm⁻¹, which can be attributed to the stretching of the C=O bond (Wang *et al.*, 2019). Additionally, peaks in the range of 1600-1681 cm⁻¹ are observed, corresponding to the stretching of C=C bonds within the aromatic ring. Another peak is observed in the range of 1483-1371 cm⁻¹, which can be attributed to the stretching of O-H and C-C bonds. Furthermore, peaks in the range of 1293-1185 cm⁻¹ are observed, indicating the stretching of C-C and C-H bonds, as well as the bending of N-H bonds (Sarkar *et al.*, 2017). Figure 1(c) displays the Fourier

Transform Infrared (FTIR) spectra of F₄ aspirin, providing evidence for the existence of a hydrogen link between the N-H and O-H bonds of F₀ and F₄ aspirin. In the case of F₀ aspirin, the peaks observed at 1628 cm⁻¹ for F₄ aspirin had a downward shift in wave number, namely to 1625 cm⁻¹. Simultaneously, the observed peak at 3235 cm⁻¹ corresponding to the stretching vibration of the O-H group experienced a shift to 3272 cm⁻¹. Additionally, the peak exhibited increased width, indicating an augmentation in hydrogen bonding. Furthermore, Ibrahim *et al.*, (2022) reported similar findings on the impact of F₁ aspirin on the establishment of robust hydrogen bonding between chitosan, CNF, and medicines. The FTIR spectrum of the composites exhibited discernible alterations, suggesting potential chemical interactions between the cellulose nanofibrils and chitosan.

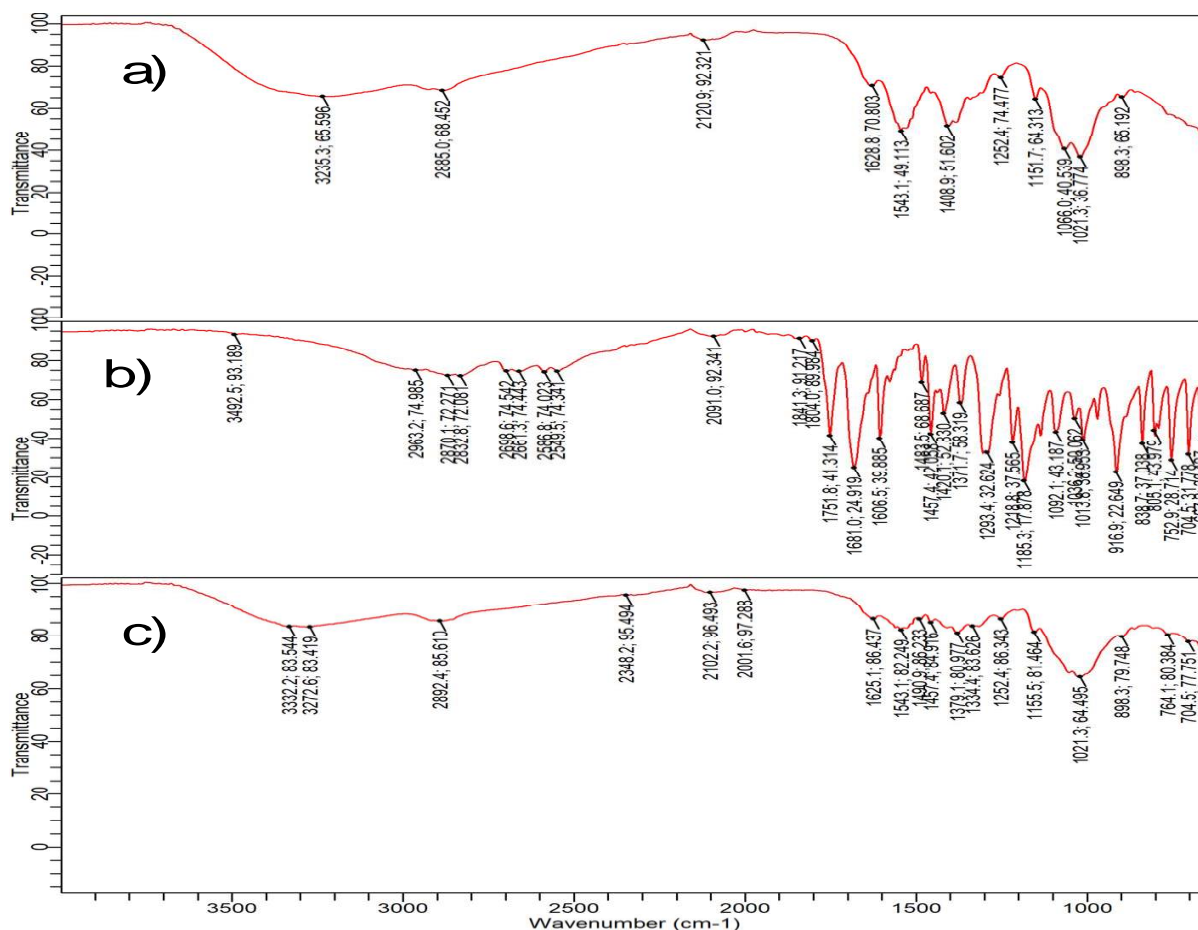


Figure 1a. Fourier Transform Infrared (FTIR) spectra of A) F₀ Aspirin, B) F₁ Aspirin, and C) F₄ Aspirin

3.2 X-ray diffraction analysis

The X-ray diffraction (XRD) pattern obtained from the composite films of chitosan-cellulose nanofibrils and aspirin exhibits distinct diffraction peaks that correspond to the crystalline phases of chitosan, cellulose, and aspirin. The observation of these peaks indicates the effective integration of aspirin into the composite films with minimal disturbance to the crystalline structure.

The X-ray diffraction (XRD) patterns obtained from the F₀, F₁, and F₄ aspirin samples exhibited peaks that were consistent with the presence of cellulose. The cellulose peaks were detected at 2θ angles of roughly 16° and 20.00°. In Figure 2(a), a prominent peak is observed at approximately 2θ = 21.3°, indicating the presence of an amorphous structure in the F₀ aspirin sample. The amorphous structures of F₁ aspirin and F₀ aspirin are evident from the presence of characteristic peaks observed at 2θ values of 21.2 and 20.03, respectively. The findings closely resemble those reported by Sarkar *et al.*, (2017).

Upon analysis of the diffractogram of CNF/chitosan composite reinforced with CNFs, it is worth mentioning that there is a noticeable drop in the intensity of the peak as the loading of CNFs increases. The observed decrease in peak intensity indicates a decline in the crystallinity of the composite material. The inclusion of nanofibrils in the chitosan matrix has the potential to disturb the overall arrangement of cellulose chains, resulting in a decrease in the crystalline nature of the composite material. The decrease in crystallinity may result in the formation of amorphous patches inside the composite material. The amorphous regions discussed in the study conducted by Ibrahim *et al.*, (2022) are characterised by the absence of a clearly defined crystal lattice structure. This structural feature results in enhanced free volume and mobility for drug molecules. Consequently, the inclusion and dispersion of pharmaceuticals inside the amorphous regions can have a significant impact on the drug release characteristics of the composites. The inclusion of amorphous areas in transdermal drug delivery systems is advantageous due to their ability to augment drug solubility and enable regulated drug release over an extended duration.

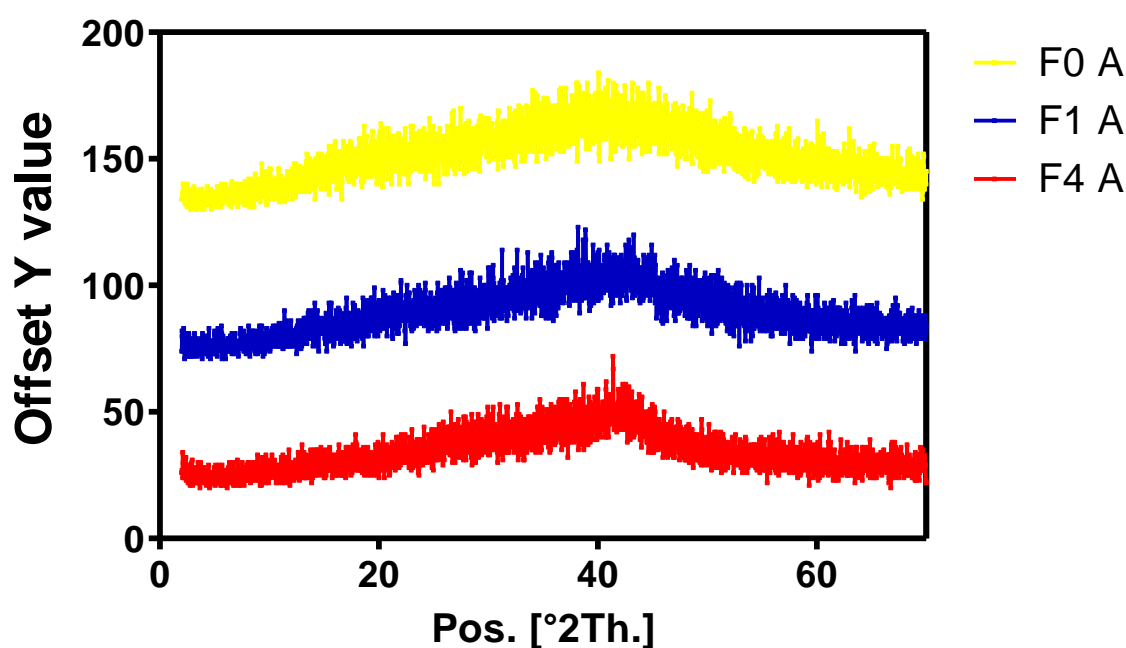


Figure 2. X-ray diffraction (XRD) diffractogram of Chitosan, Cellulose Nanofiber (CNF), F₀ aspirin, F₁ aspirin, and F₄ aspirin.

3.3 Transmission electron microscopy (TEM)

Transmission electron microscopy (TEM) is a very effective imaging technology that enables the examination of material shape and nanostructure with exceptional resolution. Figure 3 displays the transmission electron microscopy (TEM) pictures of F₀ aspirin, F₁ aspirin, and F₄ aspirin. The images reveal that the size distribution ranges from roughly 1.32 to 8.32 nm, and the composites exhibit a spherical morphology. Consistency in drug release profiles and optimisation of therapeutic efficacy are dependent on the presence of a uniform and well-defined nanofiber size. The morphologies of the particles obtained from the three formulas exhibited a predominantly spherical shape, but with some instances of aggregation.

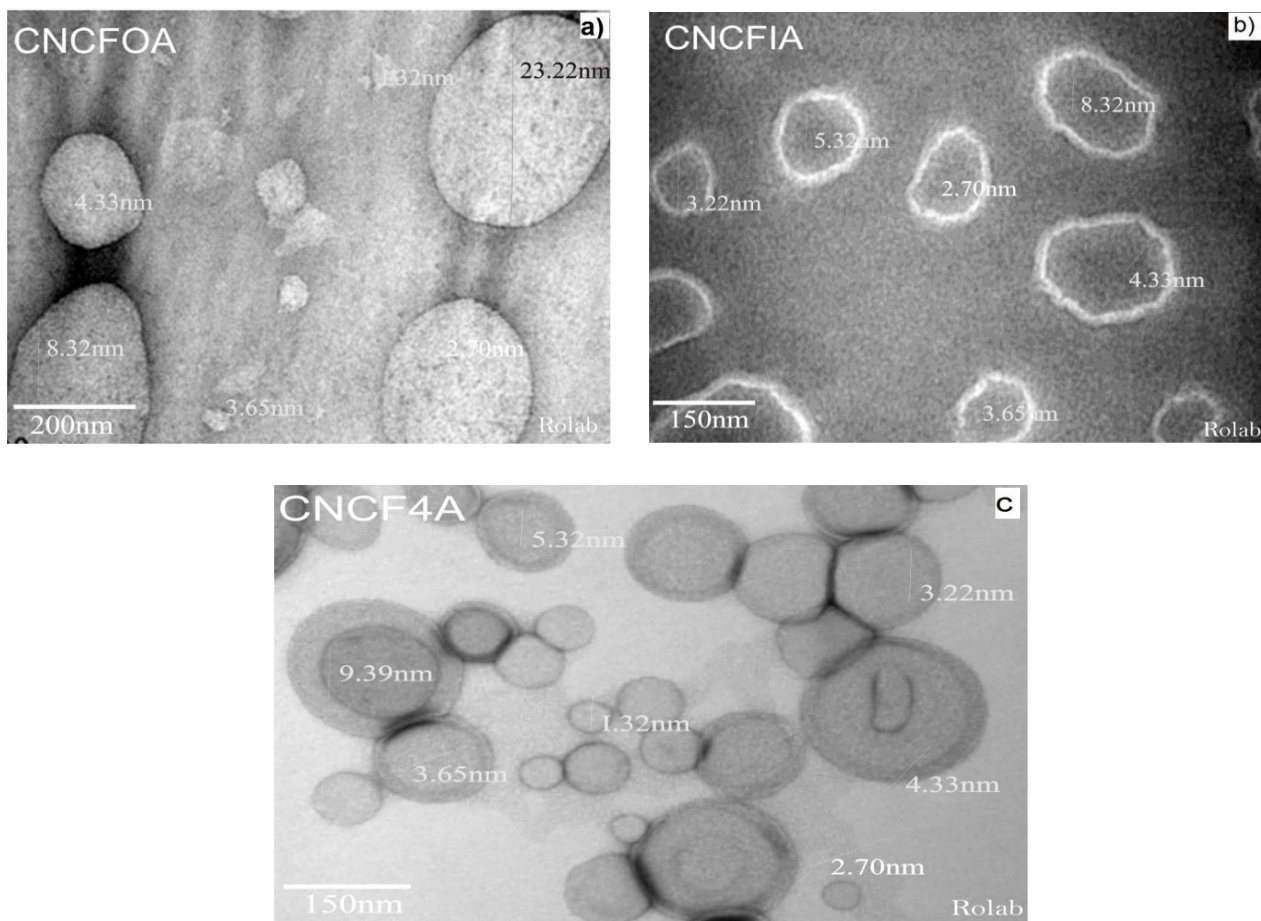


Figure 3. Transmission electron microscopy (TEM) micrographs depicting A) F₀ aspirin, B) F₁ aspirin, and C) F₄ aspirin

3.4 Differential scanning Calorimetry analysis

The utilisation of differential scanning calorimetry analysis enables the acquisition of valuable insights into the thermal characteristics and stability of the composite films. The thermogram obtained from differential scanning calorimetry (DSC) analysis of the composite films containing chitosan-cellulose nanofibrils and aspirin exhibits distinct endothermic peaks that correlate to the melting temperatures of chitosan, cellulose, and aspirin. Figure 4 displays the DSC thermograms of F₀ aspirin, F₁ aspirin, and F₄ aspirin. The DSC thermogram of F₀ aspirin, as depicted in Figure 4 (a), exhibits two distinct thermodynamic occurrences. The first event is characterised by an exothermic reaction transpiring at a temperature of 62°C. The second event is marked by a substantial endothermic peak spanning the temperature range of 90°C to 100°C, ultimately yielding a glass transition temperature (T_g) of 102°C. The occurrence of an exothermic event signifies the liberation of thermal energy from the specimen, typically linked to processes such as crystallisation, recrystallization, or other exothermic chemical reactions. The occurrence of an endothermic event signifies the uptake of thermal energy in conjunction with processes such as melting, evaporation, or other alterations in phase. The initial thermodynamic occurrence is anticipated to take place at a temperature of 62°C, signifying the release of bound water and the subsequent transformation from a rigid substance to a pliable and elastic condition. Figure 4(b) displays the differential scanning calorimetry (DSC) thermogram of F₁ aspirin, revealing two distinct thermodynamic events. The first event is characterised by an endothermic process observed at a temperature of 83°C. The second event is marked by an exothermic peak occurring within the

temperature range of 220°C to 240°C. On the other hand, the second event is associated with the deterioration of chitosan. The initial endothermic peak can be ascribed to the thermal characteristics shown by the cellulose nanofibrils. The observed peak in the given context can be attributed to the melting of the crystalline areas within the nanofibrils, which is a characteristic feature of cellulose as a semicrystalline polymer. The temperature at which the peak is observed corresponds to the melting point of the cellulose nanofibrils present in the composite material. Figure 4(c) displays the F₄ aspirin exhibiting a solitary thermodynamic occurrence, characterised by an endothermic peak observed at a temperature of 72°C. The presence of a disruptive signal within the temperature range of 260 - 300°C could perhaps be attributed to the ingress of cooler air into the measuring cell as a consequence of inadequate calibration, hence causing swings in temperature. The findings presented herein validate the thermogravimetric analysis (TGA) data.

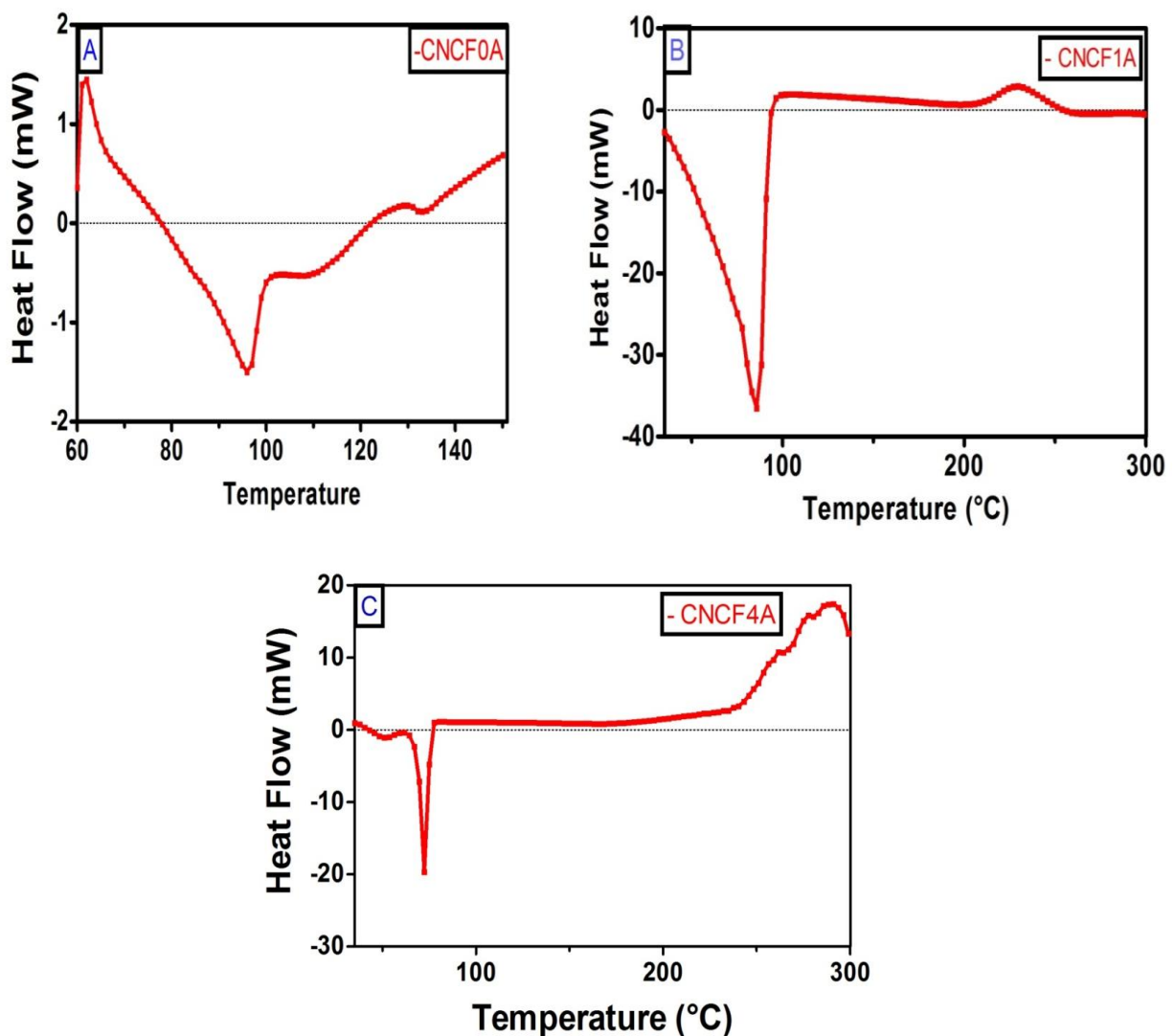


Figure 4. Differential scanning calorimetry (DSC) thermograms of three different samples: A) F₀ aspirin, B) F₁ aspirin, and C) F₄ aspirin.

3.5 Dynamic light scattering analysis

The data obtained from Dynamic Light Scattering (DLS) analysis serve as a beneficial complement to the findings obtained from Scanning Electron Microscopy (SEM), Transmission Electron Microscopy (TEM), and Differential Scanning Calorimetry (DSC) examinations. These DLS results offer

significant insights into the colloidal characteristics and stability of the composite material. Dynamic light scattering (DLS) analysis was utilised to ascertain the particle size distribution and stability of the composite films when dissolved in a solution. The suspended condition of the biopolymer cellulosic nanofibrils/chitosan composite was characterised by a well-defined particle size distribution, as determined by DLS analysis. The hydrodynamic size derived from the dynamic light scattering (DLS) findings signifies the effective size of the composite particles within the liquid medium, accounting for their interactions with the adjacent solvent molecules. The dimensions of F₀ aspirin, F₁ aspirin, and F₄ aspirin were examined using dynamic light scattering-based instrumentation, revealing sizes of 93.80 nm, 90.36 nm, and 85.79 nm, respectively. Additionally, the polydispersity index (PDI) values for F₀, F₁, and F₄ aspirin were determined to be 0.275, 0.434, and 0.403, respectively. The dimensions of F₀ aspirin exhibited a reduction upon the introduction of aspirin, resulting in a decrease to a size of 93.80nm. In a similar vein, the application of F₁ aspirin and F₄ aspirin resulted in additional reductions of 90.36 nm and 85.79 nm, respectively, when combined with the administration of aspirin and CNF. The PDI (Particle Size Distribution Index) of F₀ aspirin exhibited a substantial change, however the PDI of F₁ Aspirin and F₄ Aspirin did not demonstrate a significant change. The composite particles exhibited a hydrodynamic size falling inside the nanometer scale, aligning with the anticipated dimensions of nanofibers. The favourable aspect of the presence of minute particles lies in their ability to facilitate transdermal medication administration by promoting improved skin penetration and drug permeation through the skin barrier. Table 2 displays the dimensions, zeta potential, and polydispersity index (PDI) categories of the nanoparticles (NPs).

Table 2. Z-average and PDI of chitosan, CNF and loaded aspirin.

S/N	Composite Films	Z-average (nm)	PDI
1	Chitosan	129.7	0.425
2	CNF	107.7	0.479
3	F ₀ Aspirin	93.80	0.275
4	F ₁ Aspirin	90.36	0.434
5	F ₄ Aspirin	85.79	0.403

3.6 Thermal Analysis

Thermal gravimetric analysis (TGA) was employed to examine the thermal stability and breakdown characteristics of the composite films. The thermogravimetric analysis (TGA) curve of the composite films containing chitosan-cellulose nanofibrils and aspirin demonstrates a progressive reduction in weight as the temperature rises, suggesting the occurrence of several degradation phases. The composite films exhibited superior thermal stability compared to the separate components, indicating improved thermal characteristics.

The thermogravimetric analysis (TGA) of aspirin (F₀) exhibited three distinct phases of mass reduction. The initial phase encompasses the process of volatilization of substances, commencing from the initial temperature and extending up to approximately 280°C as shown in table 3 above. The resultant melt experiences breakdown and the ongoing elimination of volatile substances. At approximately 490 degrees Celsius. The initial phase of the weight loss regimen is characterised by a reduction of 5% in body weight, primarily attributed to the degradation of F₀.

The glass transition temperature (TG) of F₀ has a wide exothermic peak at approximately 370°C. Additionally, the endothermic transition in F₀ occurs at a lower temperature compared to CNF. The observed decrease in heat change can be ascribed to the increased number of components included in the matrix. The thermogravimetric analysis (TGA) conducted on the F₁ sample revealed the presence of three distinct phases characterised by weight reduction. The initial phase, characterised by the vaporisation of volatile molecules, occurs within a temperature range of 300°C to 390°C. This phenomenon could potentially be attributed to water depletion. The subsequent phase of weight reduction commences at a temperature of 410°C and extends until reaching 510°C, during which a substantial 80% reduction in weight is observed as a result of the degradation of F₁. The findings of the study indicate that F₁ exhibits greater thermal stability compared to F₀. The thermogravimetric analysis (TGA) of cellulose nanofibers (CNF) exhibits a wide exothermic peak at around 395°C. Isothermal conditions are observed at temperatures exceeding 550°C. The thermogravimetric analysis (TGA) of F₄ aspirin exhibited three distinct stages of weight reduction characterised by abrupt phase transitions. The initial phase encompasses the process of volatilization of substances within a temperature range of 100 to 270°C. At temperatures over 380 °C, the resultant melt experiences disintegration and a continual elimination of volatile substances. The previous weight loss series exhibited a reduction of nearly 80% in body weight, primarily attributed to the degradation of F₄. The thermogravimetric analysis (TGA) of F₄ reveals a wide exothermic peak at around 540°C.

Table 3. TGA/DTA Aspirin formulations

S/N	Composites Films	TGA/DTA Parameters (°C)		
		T _{onset}	T _{50%}	T _{degrad.}
1	Chitosan	260	510	710
2	CNF	280	395	550
3	F ₀	280	370	490
4	F ₁	300	410	510
5	F ₄	270	380	540

Conclusion

The utilization of X-ray diffraction (XRD), scanning electron microscopy (SEM), differential scanning calorimetry (DSC), dynamic light scattering (DLS), and thermogravimetric analysis (TGA) techniques has yielded significant findings regarding the production and characterization of composite films including chitosan-cellulose nanofibrils and aspirin for the purpose of drug loading. The composite films demonstrated favourable characteristics in terms of film formation, morphological stability, and thermal stability. The results of this study indicate that the composite films have the potential to serve as effective medication delivery methods. Additional research is necessary to substantiate the drug loading and release capabilities of the investigated substances, through the use of in vitro and in vivo experiments.

Acknowledgement

I am grateful to E.S Ojo from Department of Chemical Pathology, Federal Teaching Hospital Gombe, for his support during this research work.

Conflict of Interest: No conflict of interest was declared.

References

- Akartasse N., Azzaoui K., Mejdoubi E., Elansari L. L., Hammouti B., Siaj M., Jodeh S., Hanbali G., Hamed R., Rhazi L. (2022), Chitosan-Hydroxyapatite Bio-Based Composite in film form: synthesis and application in Wastewater, *Polymers*, 14(20), 4265, <https://doi.org/10.3390/polym14204265>
- Akhter N., Singh V., Yusuf M., Khan R.A. (2020), Non-invasive drug delivery technology: development and current status of transdermal drug delivery devices, techniques and biomedical applications. *Biomed Tech.* 65(3), 243–72.
- Ali H. (2017). Transdermal drug delivery system & patient compliance (2017), *MOJ Bioe quiv. Availab*, 3(2), 47–8.
- Auriema, G., Cerciello, A., Acquino, R.P. (2017), Design and development of innovative oral delivery systems. *Non-steroidal anti-inflammatory drugs*, 33.
- Bhandari, J. Mishra, H. Mishra, P.K. Wimmer, R. Ahmad, F.J. Talegaonkar S. (2017), Cellulose nanofiber aerogel as a promising biomaterial for customized oral drug delivery. *Int J Nanomedicine*, 12, 2021-2031. doi: 10.2147/IJN.S124318.
- Blanca-Lopez N., Soriano V., Garcia-Martin E., Canto G., Blanca M. (2019), NSAID-induced reactions: classification, prevalence, impact, and management strategies. *J Asthma Allergy*. 12, 217-233.
- Casettari L, and Illum L (2014), Chitosan in nasal delivery systems for therapeutic drugs. *J Control Release*. 190, 189–200.
- Du, H. Liu, W. Zhang, M. Si, C. Zhang, X. Li, B. (2019), Cellulose nanocrystals and cellulose nanofibrils based hydrogels for biomedical applications.
- El Mouaden K., El Ibrahim B., Oukhrib R., Bazzi L., Hammouti B., Jbara O., Tara A., Chauhan D. S., Quraishi M.A. (2018), Chitosan polymer as a green corrosion inhibitor for copper in sulfide-containing synthetic seawater, *International Journal of Biological Macromolecules*, 119, 1311-1323
- Gadkari, R.R., Suwalka, S., Yogi, M.R., Ali, W., Das, A., Alagirusamy, R. (2019), Green synthesis of chitosan-cinnamaldehyde cross-linked nanoparticles: characterisation, antibacterial and anti-oxidant activity. *Carbohydrate polymers*, 226,115298.
- Hammi N., Chen S., Dumeignil F., Royer S., El Kadib A. (2020) Chitosan as a sustainable precursor for nitrogen-containing carbon nanomaterials: synthesis and uses, *Materials Today Sustainability*, 10, 100053, ISSN 2589-2347, <https://doi.org/10.1016/j.mtsust.2020.100053>
- Hemmingsen L.M., Panchai P., Julin K., Basnet P., Nystad M., Johannessen M. and Škalko-Basnet N. (2022) Chitosan-based delivery system enhances antimicrobial activity of chlorhexidine. *Front. Microbiol.* 13, 1023083. doi: 10.3389/fmicb.2022.1023083
- Huang J., Deng Y., Ren J., Chen G., Wang G., Wang F., Wu X. (2018), Novel in situ forming hydrogel based on xanthan and chitosan re-gelifying in liquids for local drug delivery. *Carbohydr Polym.* 186, 54–63.
- Ibrahim, H.M., El-Bisi, M.K., Taha, G.M., El-Alfy, E.A. (2018), Preparation of biocompatible chitosan nanoparticles loaded by tetracycline, gentamycin and ciprofloxacin as novel drug delivery system for improvement the antibacterial properties of cellulose based fabrics, *International Journal of Biological Macromolecules*. <https://doi.org/10.1016/j.ijbiomac.2020.06.118>
- Liu S, Yang S, Ho PC (2018). Intranasal administration of carbamazepine-loaded carboxymethyl chitosan nanoparticles for drug delivery to the brain. *Asian J Pharm Sci* 13, 72–81.
- Lu H, Wang J, Wang T, Zhong J, Bao Y, Hao H (2016), Recent progress on nanostructures for drug delivery applications. *J Nanomater*, 2016, 20.
- Ramana L.N., Sharma S., Sethuraman S., Ranga U., Krishnan U.M (2014), Evaluation of chitosan nanoformulations as potent anti-HIV therapeutic systems. *Biochim. Biophys. Acta.* 1840:476–484.
- Sahare, P. (2018), Synthesis and Characterization of Cds. *International Journal of Engineering Research & Technology (IJERT)* ISSN: 2278-0181. Published by, www.ijert.org. NCANA – 2018. Conference Proceedings.
- Sarkar, G. Orasugh, J.T., Saha, N.R., Roy, I., Bhattacharyya, A. Chattopadhyay, A.K., Ranad, D. and Chattopadhyay, D. (2017), Cellulose nanofibrils/chitosan based transdermal drug delivery vehicle for controlled release of ketorolac tromethamine. *New J. Chem.* RCS. Pp 1-8. DOI: 10.1039/c7nj02539d
- Seah B.C., Teo B.M. (2018), Recent advances in ultrasound-based transdermal drug delivery. *Int. J. Nanomedicine*, 13, 7749–63
- Shakya A.K., Ingrole R.S.J., Joshi G., Uddin M.J., Anvari S., Davis C.M. (2019), Microneedles coated with peanut allergen enable desensitization of peanut sensitized mice. *J. Control Release*. 314, 38–47.

- Sumaila A., Sumaila A. O., Abdullahi A. S., Usman A. O., Ekwoba L. (2022), Application of chitosan-silver nanocomposites for heavy metals removal: A Review Study, *J. Mater. Environ. Sci.*, 13(8), 869-883
- Wang, F., Zhang, Q., L, X., Huang, K., Shao, W., Yao, D. and Huang, C. (2019), Redox-responsive blend hydrogel films based on carboxymethyl cellulose/chitosan microspheres as dual delivery carrier. *International Journal of Biological Macromolecules* 134. 413–421. <https://doi.org/10.1016/j.ijbiomac.2019.05.049>.
- Xing K., Zhu X., Peng X., *et al.* (2015) Chitosan antimicrobial and eliciting properties for pest control in agriculture: a review. *Agron Sustain Dev.*, 35(2), 569–588.
- Younes I. and Rinaudo M (2015), Chitin and chitosan preparation from marine sources. Structure, properties and applications. *Mar. Drugs*. 13, 1133–1174.
- Zeyadi M., Almulaiky Y. Q. (2023) Chitosan-Based metal-organic framework for Stabilization of β -glucosidase: Reusability and storage stability, *Heliyon*, 9(11), e21169, ISSN 2405-8440, <https://doi.org/10.1016/j.heliyon.2023.e21169>

(2023) ; <http://www.jmaterenvirosci.com>